

# PHYSICAL REVIEW B

## CONDENSED MATTER

THIRD SERIES, VOLUME 31, NUMBER 10

15 MAY 1985

### Photoemission study of the hydrogenation of the intermetallic compounds $YFe_3$ and $YFe_2$

H. Höchst and E. Colavita\*

*Department of Physics, University of Wisconsin—Madison, Madison, Wisconsin 53706*

K. H. J. Buschow

*Philips Research Laboratories, 5600 MD Eindhoven, The Netherlands*

(Received 27 November 1984)

Intermetallic yttrium-iron compounds do have a strong affinity to hydrogen. Exposure to  $H_2$  at 300 K leads to a hydrogen-induced state at 5.3 eV below  $E_F$  and a strong reduction of  $d$ -like states at  $E_F$ . For higher  $H_2$  exposures at 700 K, these hydrides undergo a metal-to-semiconductor transition with an energy gap  $E_0=0.3\pm 0.1$  eV. In addition to the lowering of  $d$ -like states at  $E_F$ , a second  $H_2$ -induced structure appears at 10 eV.

#### I. INTRODUCTION

The use of hydrogen as an energy carrier has led to a rapidly growing field of experimental and theoretical studies on its interaction with metals and intermetallic compounds.<sup>1-4</sup> Potential storage materials such as  $LaNi_5$  or  $TiFe$  can absorb more than twice the density of liquid hydrogen. Their surface segregation and poisoning, however, are still serious problems which limit their use as economical and rechargeable long-term hydrogen absorbers.<sup>4</sup> Moreover, the low hydrogen equilibrium pressure of many binary hydrides  $AH_2$  (with  $A=Y, Zr, Ce$ , and  $Ca$ ) excludes them as conventional storage materials.

Technologically more convenient pressure-composition isotherms can be obtained by intermetallic compounds through alloying metals with a high hydrogen affinity (rare earths,  $Y, Zr, Ti$ ) and  $3d$  elements which have nearly no affinity to hydrogen.<sup>5</sup> While the electronic properties of elemental hydrides  $AH_x$  (with  $A=Y, Zr, Hf, Er$ , and  $Pr$ ) which are formed over a wide compositional range ( $x=1-3$ ) are theoretically and experimentally well studied,<sup>6-8</sup> there is a lack of detailed understanding of the electronic properties of metal-compound hydrides.

The present work reports the first synchrotron radiation investigation on the hydrogenation of  $YFe_3$  and  $YFe_2$ . These compounds absorb hydrogen in large quantities after an initial activation obtained at higher temperatures and at a  $H_2$  pressure of 40 atm. Hydrides up to  $YFe_3H_{4.8}$  and  $YFe_2H_{4.2}$  are formed by absorption of hydrogen at 50°C.<sup>9</sup> The hydrogenation increases the lattice volume by  $\sim 20\%$  but does not change the initial crystal structure which is  $PuNi_3$  type for  $YFe_3$  and  $HgCu_2$  type for  $YFe_2$ .<sup>5</sup> The low hydrogen equilibrium pressure which is less than  $10^{-5}$  atm allows an *in situ* study of

the early stages of hydride formation in an ultrahigh vacuum.

#### II. EXPERIMENTAL

The samples were prepared by arc-melting followed by annealing under vacuum. X-ray diffraction with monochromatized  $CuK_\alpha$  radiation was used to determine their crystallographic structure and homogeneity. Samples were exposed to  $H_2$  atmosphere in the  $10^{-4}$ – $10^{-7}$ -Torr range at different temperatures between 300 and 700 K.

The photoemission measurements were performed using synchrotron radiation from the electron storage ring Tantalus of the University of Wisconsin, Madison. The radiation was dispersed with an ultrahigh-vacuum grasshopper monochromator. The base pressure of the vacuum chamber during each run was in the  $10^{-11}$ -Torr range. Photoelectron energy analysis was carried out with a double-pass cylindrical mirror analyzer (CMA) used in the angle-integrated mode. The total energy resolution (monochromator and analyzer) was experimentally determined from the width of the photoemission onset at the Fermi level to be  $\sim 0.35$  eV.

The samples were cut in the form of plates of  $5\times 4\times 1$  mm<sup>3</sup> and were mounted so that their surface normal was at an angle of 42° with respect to the CMA axis and the angle of incidence at  $\sim 30^\circ$  with respect to the sample surface.

Surface contamination has been removed by bombardment with Ar ions at an energy of 500 eV. After several hours of cleaning, well-developed oxide-free core lines of Y and Fe have been measured at  $E_B(Y 4p_{3/2})=26.1(3)$  eV,  $E_B(Fe 3p)=52.8(3)$  eV, and  $E_B(Fe 3s)=91.8(3)$  eV. The valence band spectra showed, however, small amounts of Ar 3p emission at 11 eV which could be re-

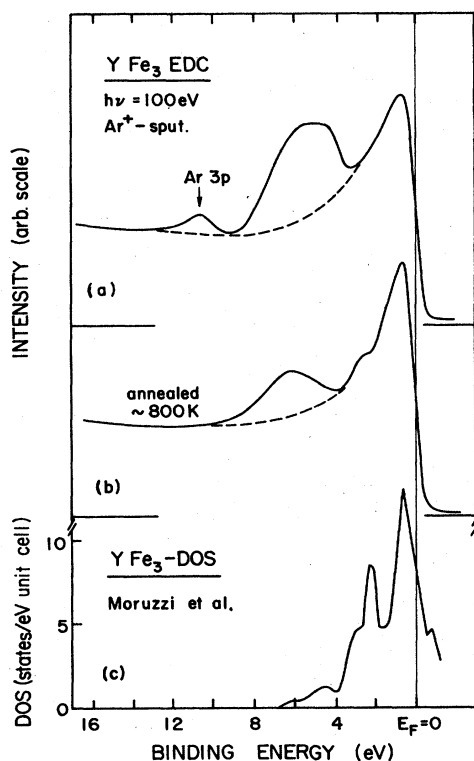


FIG. 1. (a) Valence band photoemission spectra of  $\text{YFe}_3$  obtained at  $h\nu=100$  eV after sputtering with Ar ions of 500 eV kinetic energy. (b) Valence band EDC after annealing at 300 K for 10 min. (c) Total density of states of  $\text{YFe}_3$  from Ref. 10.

moved by an annealing of the samples for 15 min at  $\sim 600$  K.

### III. RESULTS AND DISCUSSION

#### A. Hydrogen-induced features: Low coverage

The valence band energy distribution curves (EDC) of  $\text{YFe}_3$  obtained at  $h\nu=100$  eV are shown in Figs. 1(a) and 1(b) after each step of the cleaning procedure. The annealing of the sample narrows and reduces the intensity of the broad structure of  $\sim 5.3$  eV of binding energy and, moreover, makes a new feature at  $\sim 2.5$  eV appear. Since the ratio of intensities of Y 4p and Fe 3p core lines does not change with prolonged sputtering, a preferential sputtering mechanism leading to a substoichiometric surface composition can be excluded.

After several cleaning cycles, the Y 4p core line spectrum does not show additional oxide structures. Since the photoemission cross section at low photon energy is bigger for O 2p than that of Y 4p and Fe 3p, we still cannot completely rule out the possibility that the 5.3-eV feature is related to O 2p emission. Reduction of the surface oxide by heating the samples at elevated temperatures in a  $\text{H}_2$  atmosphere did not remove this valence band structure but increased it further. Since the intensity of the 5.3-eV structure increased with  $\text{H}_2$  exposures, it is more likely a  $\text{H}_2$ -induced feature. Moreover, this structure is not relat-

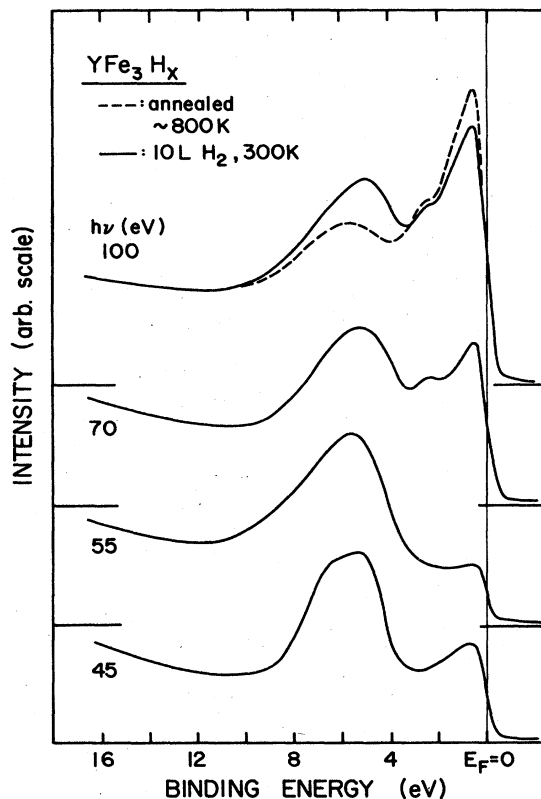


FIG. 2. Valence band EDC's of  $\text{YFe}_3$  after exposure to 10-L  $\text{H}_2$  at 300 K obtained with different photon energies. [1 langmuir (L)  $\equiv 10^6$  Torr sec.]

ed to  $\text{YFe}_3$  valence band emission as can be seen by comparison with theoretical calculations.<sup>10</sup>

The total density of states (DOS) of pure  $\text{YFe}_3$  calculated by Moruzzi *et al.*,<sup>10</sup> shown in Fig. 1, reproduces the peaks at 0.5 and 2.5 eV below  $E_F$  whereas the structure at 5.3 eV has no counterpart. However, it is close to the bottom of the valence band and the theoretical DOS exhibits a weaker third structure around 4–6.5 eV below  $E_F$ . The small DOS in this region is due to *s-p*-like bands while the high DOS around  $E_F$  arises mainly from electrons having *d*-band character. Thus the different partial photoionization cross sections for *s-p*- and *d*-like states should produce a much less intense emission around 6 eV.

Although the theoretical comparison has been limited to  $\text{YFe}_3$ , it can also be extended to  $\text{YFe}_2$  since band structure calculations<sup>11</sup> using a tight binding approximation reveal a total *d*-band DOS for  $\text{YFe}_2$  which is similar to that of  $\text{YFe}_3$ .

The high affinity of Y-based 3d compounds to hydrogen supports further the conclusion that the 5.3-eV structure is related to hydrogen-derived bands. Similar structures have been observed in synchrotron radiation<sup>6</sup> and x-ray photoemission experiments<sup>7,8</sup> on *d*-band metal hydrides. Small  $\text{H}_2$  contaminations of the vacuum system which cannot be avoided easily do result in an early stage of the formation of  $\text{YFe}_3$  hydrides.

The reaction of hydrogen with  $\text{YFe}_3$  is shown in the upper part of Fig. 2. In comparison with the annealed sample, exposure to 10-L  $\text{H}_2$  leads to a reduction of *d*-

state emission at  $E_F$  and to a further increase of the 5.3-eV structure.

### B. Resonance effect

Valence band photoemission spectra taken at different photon energies do show similar structures but with different relative intensities (Fig. 2). At  $h\nu=55$  eV the intensity of the peak at 0.5 eV below  $E_F$  goes through a minimum. The shoulder at  $\sim 2.5$  eV below  $E_F$  weakens and cannot be resolved at photon energies below  $h\nu < 70$  eV.

Intensity modulations of the valence band emission are quite common and have been observed for  $d$ - and  $f$ -band metals.<sup>12-14</sup>

The effect of resonant photoemission can be used as a spectroscopic tool to determine the angular character of the local valence band DOS.<sup>15</sup> The strong resonant reduction of emission at  $E_F$  can be used to investigate the changes in the  $d$ -like DOS at different stages of hydrogenation. For compounds containing  $3d$  metals the excitation of a  $3p$  core level gives rise to a discrete excited  $3p^5 3d^{N+1}$  state which may decay, via a super-Coster-Kronig (SCK) transition, into a continuum  $3p^6 3d^{N-1} \epsilon_f$  final state. Since the direct valence band photoemission  $3p^6 3d^N + h\nu \rightarrow 3p^6 3d^{N-1} \epsilon_f$  leads to the same final state both channels may interfere and give rise to resonances or antiresonances in the photoemission cross section.<sup>16</sup>

Figure 3 shows the resonance effect at  $h\nu \sim 55$  eV for the  $YFe_3$  which had been exposed to 10-L  $H_2$  at room temperature. The intensities of the valence band structure at initial energy  $E_i = 0.5$  eV below  $E_F$ , which had been normalized with respect to the intensity of the EDC's at 15 eV, shows a well-developed dip at  $h\nu \sim 55$  eV. The choice of the reference point at 15 eV of binding energy has been used since it is not affected either by valence band structures or the onset of additional Auger emission. Thus it can be used to correct the valence band intensities

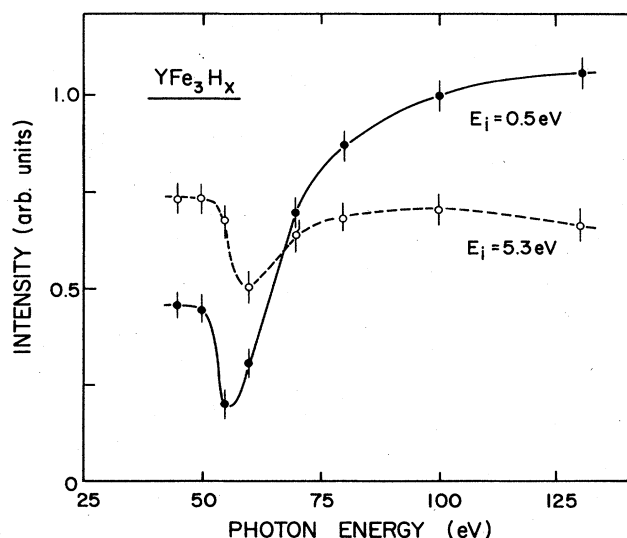


FIG. 3. Photon energy dependence of the emission at  $E_i = 0.5$  and 5.3 eV below  $E_F$  for  $YFe_3$  exposed to 10-L  $H_2$  at 300 K.

against the monochromator response function.

The normalized EDC intensity at  $E_i = 5.3$  eV shows an analogous but weaker resonant effect. The amplitude of the EDC at  $E_i = 5.3$  eV has been corrected against the inelastic background by assuming a linear increase from  $E_F$  up to the tail of secondary electrons.

Since both initial states ( $E_i = 0.5$  and 5.3 eV) resonate around the Fe  $3p$  threshold they have to be of  $d$  symmetry. The weaker resonance at  $E_i = 5.3$  eV can be explained by a less-pronounced  $d$ -like character of the hydrogen-induced EDC structure.

### C. Metal to semiconductor transition

The effects of higher hydrogen exposures to  $YFe_2$  are shown in Fig. 4. Valence band EDC's are taken around the resonance energy at  $h\nu = 55$  eV and at  $h\nu = 100$  eV. The spectra are very similar to those obtained for  $YFe_3$  after the equivalent  $H_2$  exposure as expected from the similarity of the main features<sup>10,11</sup> between  $YFe_3$  and  $YFe_2$  DOS's.

Room-temperature adsorption is saturated after an exposure to 10 L of  $H_2$ . A further change in the valence band EDC can be obtained by exposures at higher temperatures. The 5.3-eV peak sharpens and increases considerably after an exposure at  $10^3$  L of  $H_2$  at 700 K while the emission due to the region close to  $E_F$  is strongly re-

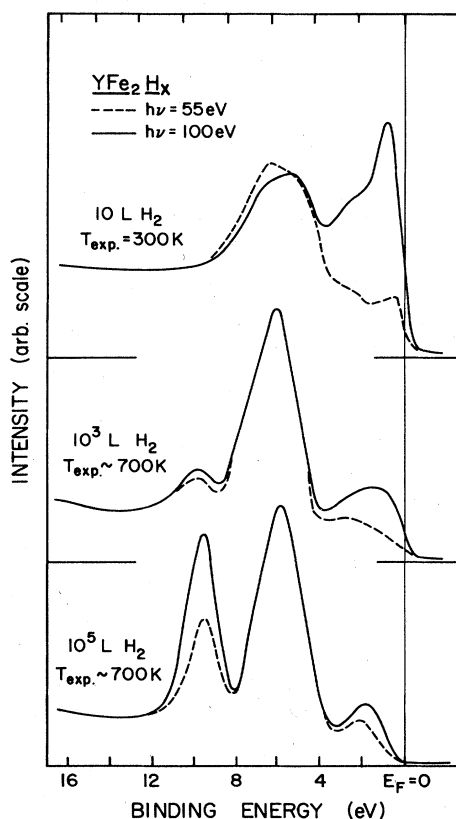


FIG. 4. Valence band EDC's of  $YFe_2$  at different stages of hydrogenation obtained at photon energies of  $h\nu = 55$  eV (dashed line) and  $h\nu = 100$  eV (solid line).  $T_{exp}$  indicates the temperature at which the sample has been exposed to hydrogen.

duced and a new structure arises at 10 eV of binding energy. The comparison between the spectra taken around the resonance energy ( $h\nu=55$  eV) and out of resonance ( $h\nu=100$  eV) show that  $d$ -like states have been drastically removed from  $E_F$ . Both effects, the decrease of  $d$ -like state at  $E_F$  and the filling of a new state at  $\sim 10$  eV, increase further with higher hydrogen exposures.

The electronic properties of the sample changed with increasing hydrogenation from metallic to semiconductor behavior. Extrapolating from the top of the valence band emission, we obtain an energy gap  $E_0=0.3\pm 0.1$  eV for the highest  $H_2$  exposure by assuming that  $E_F$  is located at the bottom of the conduction band.

A metal to semiconductor transition<sup>2,17</sup> has been predicted for the system  $YH_x$  with  $x\sim 2.8$  by Switendick.<sup>2</sup> Since there is the lack of proper theoretical calculations of intermetallic compound hydrides we will use arguments in analogy to those describing the electronic properties of elemental hydrides.<sup>2,3,17-19</sup>

These theories predict that each H atom which is inserted into the unit cell will form a new band below the bands with predominant metal  $d$  character. Due to the hybridization of these hydrogen-induced states with metal  $d$  states, these new bands will have also some  $d$  character. Thus for the dihydrides, two hydrogen-induced bands form below the  $d$  bands and accommodate four of the five valence electrons. Since the fifth valence electron partially fills the metal  $d$  bands, the dihydride is metallic. Consequently, the trihydride will have a semiconductor behavior because the three-hydrogen-induced bands accommodate all of the six valence electrons.

The hydrogen-induced effects, the removal of  $d$ -like states around  $E_F$ , and the formation of a new structure at  $\sim 5.3$  eV below  $E_F$ , which are seen in the valence band spectra of  $YFe_2$  and  $YFe_3$  during the different stages of hydrogenation, are similar to those of elemental hydrides whereas the appearance of a third peak at 10 eV below  $E_F$  seen for higher exposures has no counterpart in elemental hydrides.

Since elemental hydrides do undergo different phase transitions with different hydrogen occupation sites, whereas yttrium-iron hydrides do not change their crystal structure, it may not be appropriate to compare the electronic structure of these two systems at least for higher hydrogen concentrations.

For the understanding of these problems a detailed theoretical analysis seems to be necessary. The ability of yttrium-iron compounds to form stable hydrides up to  $YFe_2H_{4.8}$  around room temperature cannot easily be explained either by the high  $H_2$  affinity of Y or by its contribution to the electronic properties of the compound. Actually, local density-of-states calculations<sup>11</sup> of  $YFe_2$  do show only a negligible amount of Y  $d$  states within the first few eV below  $E_F$ .

#### IV. CONCLUDING REMARKS

Ternary hydrides of the type  $MFe_2H_x$  were obtained for various hydrogen concentrations by Viccaro *et al.* and their magnetic properties studied by  $^{57}Fe$  Mössbauer spectroscopy.<sup>20</sup> Their results showed that  $H_2$  absorption leads to an increase in the Fe magnetic moment up to a  $H_2$  concentration of  $x\sim 3.7$ . For  $x > 3.7$  the magnetic moment decreased drastically. The result of the present photoemission study correspond closely to this behavior since the prerequisite for the formation of the  $3d$  moment, i.e., the high  $d$ -like density of states at  $E_F$ , was shown to be absent in the case of high  $H_2$  exposures.

However, the pressure composition isotherms of  $YFe_2H_x$  and  $YFe_3H_x$  are such that the bulk hydrogen content must be considered to be low under the present experimental condition.<sup>21</sup> For this reason we are led to the conclusion that features observed in the valence band spectra reflect mainly hydrogen-induced changes close to the surface region of the samples.

Besides the theoretically expected behavior of a metal to semiconductor transition with increasing  $H_2$  content we observed a new strong feature at  $\sim 10$  eV below  $E_F$  in the valence bands of  $YFe_2$  and  $YFe_3$  after high  $H_2$  exposures.

The appearance of a second hydrogen-induced metal band cannot be explained within the anion model proposed by Switendick<sup>2</sup> to explain the band structure of binary hydrides. It seems that at higher  $H_2$  contents the so called proton model which assumes charge transfer from the hydrogen to metal  $d$  states, and as a result of this a splitting of metal states, is more appropriate to describe the electronic structure of ternary hydrides. It should be recalled that the hydrogen content of the ternary hydrides ( $YFe_2H_{4.2}$  and  $YFe_3H_{4.8}$ ) when expressed as the number of H atoms per Y atom is considerably larger than that of  $YH_3$  for instance.

Further experiments are planned including an investigation of the core line shifts during the hydrogenation stages as well as the quantitative determination of the absorbed hydrogen. Studies will also focus on the so-called activation treatment of the compounds. Since this is generally a procedure necessary to initiate the high room-temperature  $H_2$  uptake, it seems to be a crucial step controlling the  $H_2$  dissociation at the surface and diffusion into the bulk.

#### ACKNOWLEDGMENTS

This work was partly supported by General Motors Research Laboratories. One of the authors (E.C.) was supported by an International NATO grant of the National Research Council of Italy. We gratefully acknowledge the friendly assistance of the staff of the Synchrotron Radiation Center of the University of Wisconsin, Madison.

\*On leave from Department of Physics, University of Calabria, Arcavacata di Rende, I-87036 Cosenza, Italy.

<sup>1</sup>G. Alefeld and J. Völkl, *Hydrogen in Metals* (Springer, Berlin, 1978), Vol. 1.

<sup>2</sup>A. C. Switendick, *Solid State Commun.* **8**, 1463 (1970); *J. Less-Common Met.* **74**, 199 (1980).

<sup>3</sup>D. J. Peterman, B. N. Harmon, J. Marchiando, and J. H. Weaver, *Phys. Rev. B* **19**, 4867 (1979).

- <sup>4</sup>H. C. Siegman, L. Schlapbach, and C. R. Brundle, *Phys. Rev. Lett.* **40**, 972 (1978).
- <sup>5</sup>K. H. J. Buschow and P. F. de Châtel, *Pure Appl. Chem.* **52**, 135 (1979).
- <sup>6</sup>J. H. Weaver, D. J. Peterman, D. T. Peterson, and A. Franciosi, *Phys. Rev. B* **23**, 1692 (1981).
- <sup>7</sup>A. Fujimori and L. Schlapbach, *J. Phys. C* **17**, 341 (1984).
- <sup>8</sup>A. Fujimori and J. Osterwalder, *J. Phys. C* **17**, 2869 (1984).
- <sup>9</sup>R. H. van Essen and K. H. J. Buschow, *J. Less-Common Met.* **70**, 189 (1980).
- <sup>10</sup>V. L. Moruzzi, A. R. Williams, A. P. Malozemoff, and R. J. Gambino, *Phys. Rev. B* **28**, 5511 (1983).
- <sup>11</sup>H. Yamada, J. Inone, K. Terao, S. Kanda, and M. Shimizu, *J. Phys. F* **14**, 1943 (1984).
- <sup>12</sup>C. Guillot, Y. Ballu, J. Paigné, J. Lecante, K. P. Jain, P. Thiry, R. Pinchaux, Y. Petroff, and L. M. Falicov, *Phys. Rev. Lett.* **39**, 1632 (1977).
- <sup>13</sup>H. Höchst and M. K. Kelly, *Phys. Rev. B* **30**, 1708 (1984).
- <sup>14</sup>B. Reihl, N. Mårtensson, D. E. Eastman, A. J. Arko, and O. Vogt, *Phys. Rev. B* **26**, 1842 (1982).
- <sup>15</sup>R. D. Bringans and H. Höchst, *Phys. Rev. B* **30**, 5416 (1984).
- <sup>16</sup>L. C. Davis and L. A. Feldkamp, *Phys. Rev. B* **23**, 6239 (1981).
- <sup>17</sup>D. K. Misemer and B. N. Harmon, *Phys. Rev. B* **26**, 5634 (1982).
- <sup>18</sup>J. H. Weaver, R. Rosei, and D. T. Peterson, *Phys. Rev. B* **19**, 4855 (1979).
- <sup>19</sup>J. H. Weaver, D. T. Peterson, and R. L. Benbow, *Phys. Rev. B* **20**, 5301 (1979).
- <sup>20</sup>P. J. Viccaro, G. K. Shenoy, B. D. Dunlap, D. G. Westlake, and J. F. Miller, *J. Phys. (Paris) Colloq.* **40**, C2-198 (1979).
- <sup>21</sup>H. A. Kierstead, *J. Less-Common Met.* **70**, 199 (1980).